ELSEVIER

Wear 250 (2001) 718–725

WEAR

www.elsevier.com/locate/wear

A study on wear coefficients and mechanisms of steam generator tube materials

Young-Ho Lee [a], In-Sup Kim [a,*], Sung-Sik Kang [b], Hae-Dong Chung [b]

[a] *Korea Advanced Institute of Science and Technology, 373-1 Kusong-dong, Yusong-gu, Taejon 305-701, South Korea*
[b] *Korea Institute of Nuclear Safety, 19 Kusong-dong, Yusong-gu, Taejon 305-338, South Korea*

Abstract

Reciprocating sliding wear tests were performed to evaluate wear properties of Inconel 600MA and 690TT steam generator (SG) tube materials against 405 and 409 ferritic stainless steels. With increasing normal loads and sliding amplitudes, the wear rate of tube materials increased but a wear transition occurred only in Inconel 690TT. Subsurface deformation strengthening seemed to be an important factor that determines the wear resistance of tube materials. After the wear test, the worn surfaces were observed to investigate the wear mechanism of tube materials using SEM. The results indicated that there are different mechanisms of wear particle removal between the tube materials. The differences are related to the degree of work hardening due to the differences in chromium content in the tube materials. Based on the present results, wear coefficient values for the life estimation of SG tubes were calculated according to the work-rate model at each test condition. The wear rate is lower for Inconel 690TT compared to that for Inconel 600MA. Finally, parameters that should be considered for evaluation of wear coefficients were discussed.

Keywords: Steam generator tube; Work-rate model; Inconel 600MA; Inconel 690TT; Wear coefficient; Ferritic stainless steel

1. Introduction

Fretting wear damage of steam generator (SG) tube materials is now one of the most severe degradation mechanisms, which is caused by flow-induced vibration between tube and support materials. Flow-induced vibration occurs due to high flow rates and small clearance between tubes and their supports. It is impossible to remove completely the tube vibration at supporting places, so some form of wear phenomenon always exists in SG. Therefore, many nuclear power plants reported fretting-related leaking and especially tubes rupture occurred in Palo Verde and Mihama. Recently, there has been much improvement of corrosion resistance of SG tube after tube material replacement of Inconel 600MA with Inconel 690TT or improvement of water treatment [1]. However, there are not enough investigations about wear properties of tube materials such as Inconel 600MA and 690TT.

Experimental studies on fretting wear in SG tube materials have been performed since early 1970s [2] and proposed many semi-empirical models to predict the tube wear damage. Recently, a work-rate model has been proposed by Frick et al. [3] and widely used as the fretting wear model in SG tube materials. To reduce the wear damage in tube materials, wear mechanisms must be examined at various test variables such as applied normal load, sliding amplitude, temperature, counter part materials, etc. In many research papers about the fretting wear of SG tubes [4–6], the aims of studies have been focused on the evaluation of wear coefficients at each test conditions in the view of life estimation. To understand the wear characteristics of SG tube materials, SG wear model must be considered for the evaluation not only of wear coefficient, but also of the wear mechanism of the contact surfaces.

The objectives of this study are to compare the wear mechanism of SG tube materials against ferritic stainless steels and to evaluate wear coefficients from the work-rate model. The role of wear particles generated from work-hardened layer and of chromium content in subsurface hardening is to be examined.

2. Experimental procedure

2.1. Wear specimen

Specimens of Inconel 600MA and 690TT SG tubes (abbreviated to 600MA and 690TT), 19.05 mm diameter by 14 mm long, were cut from the straight tube and support specimens of 405 and 409 stainless steels (abbreviated to 405SS and 409SS) were prepared from the flat strip. Chemical composition of tube and support materials is shown in Table 1. The weight loss of specimens was obtained

* Corresponding author. Tel.: +82-428693815; fax: +82-428693810.

0043-1648/01/$ – see front matter
PII: S0043-1648(01)00680-9

Table 1
Chemical compositions of wear tested materials (wt.%)

Specimen	Cr	Fe	C	Si	Mn	Ti	P	S	Co	Ni
600MA	16.81	9.1	0.026	0.32	0.81	0.35	0.008	0.002	0.012	Balance
690TT	29.5	10.4	0.02	0.33	0.26	0.32	0.004	0.001	0.012	Balance
405SS	11.5–14.5	Balance	0.08	1.00	1.00	0.1 (Al)	0.04	0.03	–	–
409SS	10.5–11.75	Balance	0.08	1.00	1.00	6×%C	0.045	0.045	–	–

Table 2
Mechanical properties of Inconel 600MA, 690TT, 405 and 409 stainless steel

Specimen	Yield stress (MPa)	Tensile strength (MPa)	Elongation (%)	Hardness (HV)
600MA	283.5	682.6	47.3	194
690TT	316.5	708.7	46	193
405SS	170	415	20 (min)	215
409SS	205	415	20 (min)	229

by weighing before and after experiments on an analytical balance with accuracy in the order of 0.1 mg. Specimen was cleaned with acetone in an ultrasonic bath and then, dried in compressed air. To minimize errors in weighing, average values from several measurement and reference specimen were used. Tensile properties and microhardness are shown in Table 2. Microhardness (HV) values were measured with 50 g weight.

2.2. Test machine and variables

To simulate fretting wear phenomenon between tube and their support materials, reciprocating wear apparatus with tube-on-plate configuration has been developed as shown in Fig. 1. Applied normal load and sliding amplitude, that were important variables in wear testing, were continuously being monitored during testing, and frequency was controlled by motor speed. The tube specimen oscillated with a peak-to-peak amplitude of 15–40 μm at a frequency of 30 Hz. The applied normal loads were ranged from 10 to 22 N. Test environment was air at room temperature. As increasing testing cycles, contact area increased and contact load decreased. To keep up constant load level, the applied normal load was compensated within ±7% of the mean value manually during experiments.

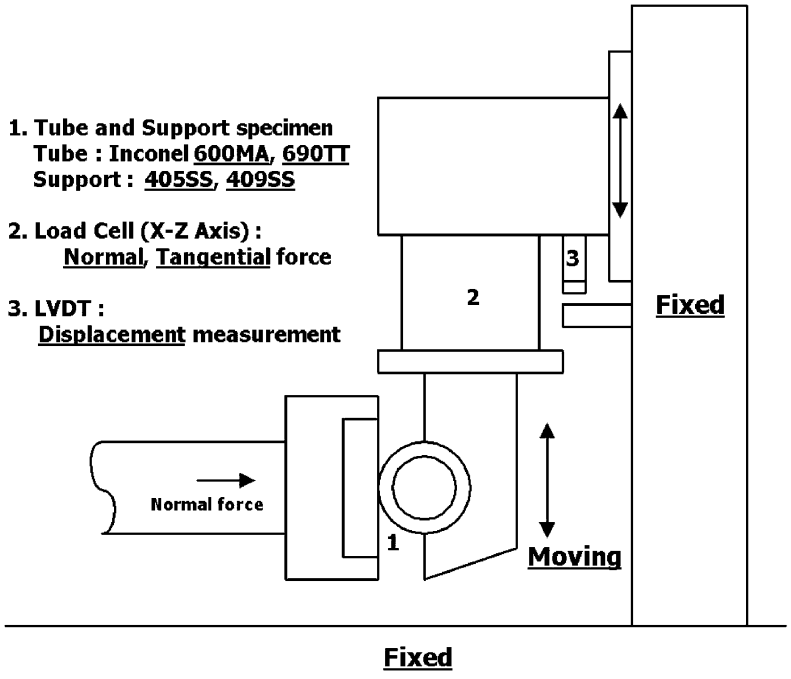

Fig. 1. Schematic diagram of the reciprocating sliding wear test machine.

2.3. Worn surface examination

To compare wear mechanisms between tube materials, worn surface was examined using SEM after wear testing. Prior to SEM examination, wear surfaces are acoustically cleaned in ultrasonic bath and removed almost all wear debris or loose particles. Generally, it is difficult to perform the real-time observation of wear mechanism in sliding wear. In this study, wear particles generated during reciprocating sliding wear testing were collected and observed the deformation characteristics on the worn surface. These particle morphologies were compared with the results of worn surface examination.

2.4. Application of the work-rate model

Many researchers proposed various semi-empirical models of modifying the Archard wear equation. Frick proposed the modified wear equation and a work-rate model. The work-rate model has been widely used to evaluate and estimate wear damage in SG tubes. From the results of wear testing, the wear coefficients of work-rate model was calculated and proposed a fretting wear curve for each test condition.

3. Results and discussion

3.1. Effect of applied normal load and sliding amplitude

Figs. 2 and 3 show the effect of the normal loads and sliding amplitudes on the mass loss of the tube materials. Generally, wear volume is linearly depending on the applied normal load and sliding distance. In 600MA, mass loss linearly increased with the applied normal load and sliding amplitude, and it was little dependent on the condition of each support materials. In the contrast to the 600MA tubes, mass loss does not change above the applied normal load of 15 N and sliding amplitude of 30 μm in 690TT tubes. Generally, the contact area of tube specimen and interaction of asperities increased with increasing of normal load and sliding amplitude. Therefore, relatively slow wear rate in 690TT is related to the characteristics of wear particle layer. Based on the study on the development of wear-protective load-bearing layers on the wear surfaces, Jiang proposed that these changes of wear rate are closely associated with the formation of oxidized or, at least partially oxidized, load-bearing layers on the wear surfaces [7]. The effects of applied work (applied normal load times sliding distance) on mass loss are shown in Fig. 4. Wear volume is a function of applied normal load times sliding distance at various wear equation. The results of this experiment shows that the wear rate does not linearly increased with increasing applied work, especially in 690TT.

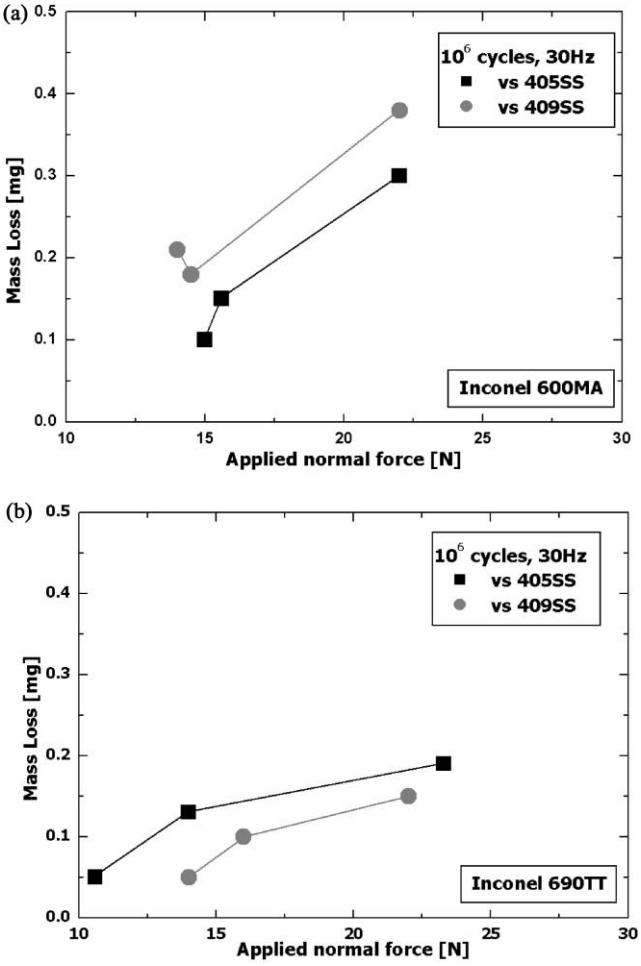

Fig. 2. Results of mass loss vs. applied normal load for the four material combinations: (a) Inconel 600MA vs. ferritic stainless steel; (b) Inconel 690TT vs. ferritic stainless steel.

3.2. Worn surface examination

To investigate the effects of test variables and the deformation behavior on the surface, worn surface observations were performed using SEM after acoustic cleaning in ultrasonic bath and results are shown in Fig. 5. In 600MA, the formation of deformation wedges were dominant after they were generated at contact surface due to the severe shear plastic deformation. The fine tracks seemed to be generated due to the fine particles during abrasive wear, and they were observed in surroundings of deformation wedges. These morphologies of worn surface were mostly appeared in 600MA in both tube support materials. In 690TT, worn surfaces were flat and had much cracks in contrast to 600MA. Fine wear particles were still adhered to worn surface even after ultrasonic cleaning. The fine tracks that appeared in 600MA were not found in 690TT.

The wear particle layers were observed as shown in Fig. 6. In 600MA, wear particle layers were rarely observed. But severe deformed layers on the worn surface were clearly

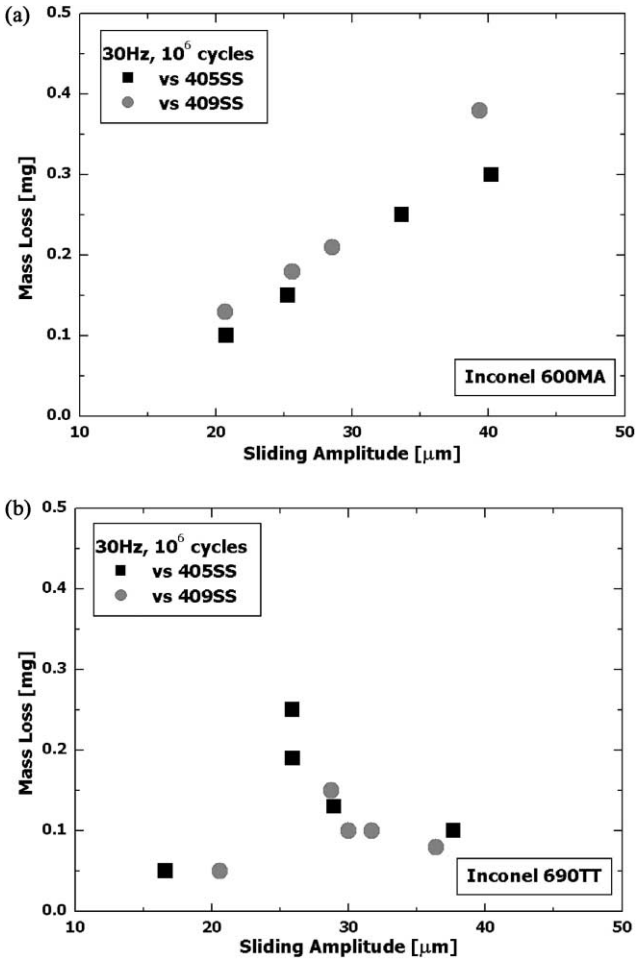

Fig. 3. Effect of sliding amplitude on wear rates: (a) Inconel 600MA vs. ferritic stainless steel; (b) Inconel 690TT vs. ferritic stainless steel.

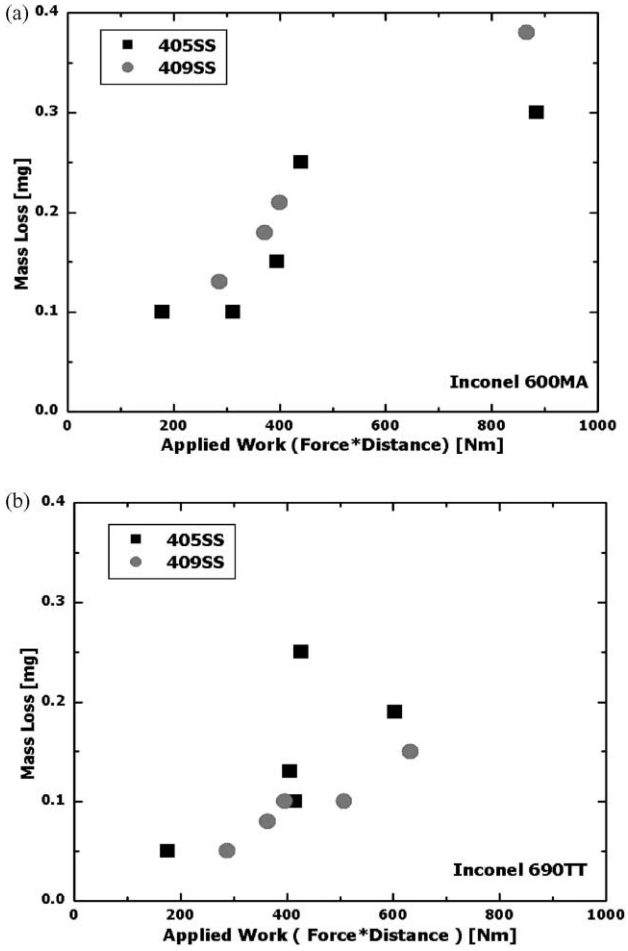

Fig. 4. Effect of applied work on wear rate: (a) Inconel 600MA vs. ferritic stainless steel; (b) Inconel 690TT vs. ferritic stainless steel.

appeared and fine cracks were observed. Due to the fine crack propagation, wear layers were separated from matrix. On the other hand, wear particle layers were observed in 690TT, which were generated from the agglomeration of wear debris. These layers were more resistant to sliding wear and seemed to act as load-bearing layers [8].

As shown in Fig. 5, generations and fractures of these layers in 600MA seem to continuously occur with increasing cycles. So, the fractured particle layers became more and more fine wear particles and these particles are trapped on the suitable sites of contact material surfaces or escaped from the contact areas. As the reciprocating sliding continues, trapped fine particles are subjected to compressive stress. Therefore, these trapped fine wear particles are compacted on the worn surface and build up the wear protective layers after their contact surroundings are worn down. Nevertheless, from the results of worn surface examination, these compacted particle layers are turned out to be not strongly adhered to the worn surface. Especially, the absorption of wear particles between the compacted particle layer and the worn surface is relatively weak. Due to these isolated particles, abrasive wear occurred on the worn surface and these traces clearly appears in Fig. 5. In 690TT, the mechanism of wear particle generations at the early stage is similar in 600MA. But SEM observation indicated that fine wear particles were agglomerated on the worn surfaces and formed the solid layer similar to the products of fine particle sintering process. Because these solid layers are strongly adhered to the worn surface, it is very difficult to remove these compacted layers during sliding testing. Besides, these layers were not removable even after the ultrasonic cleaning. Thus, these layers seem to be act as wear-protective layers during they come into contact with support materials. From the results of Jiang's study [7], he proposed that wear transition phenomenon is closely related with the development of wear-protective layers. Therefore, the lower wear rate in 690TT is related to the compact layers generated on the worn surface, which seem to reduce the friction of contact interface.

To evaluate the properties of wear debris particles, energy dispersive spectrometer (EDS) analysis were performed at each test conditions. The wear particles were mainly fine black powder in the final stages of reciprocating sliding. The

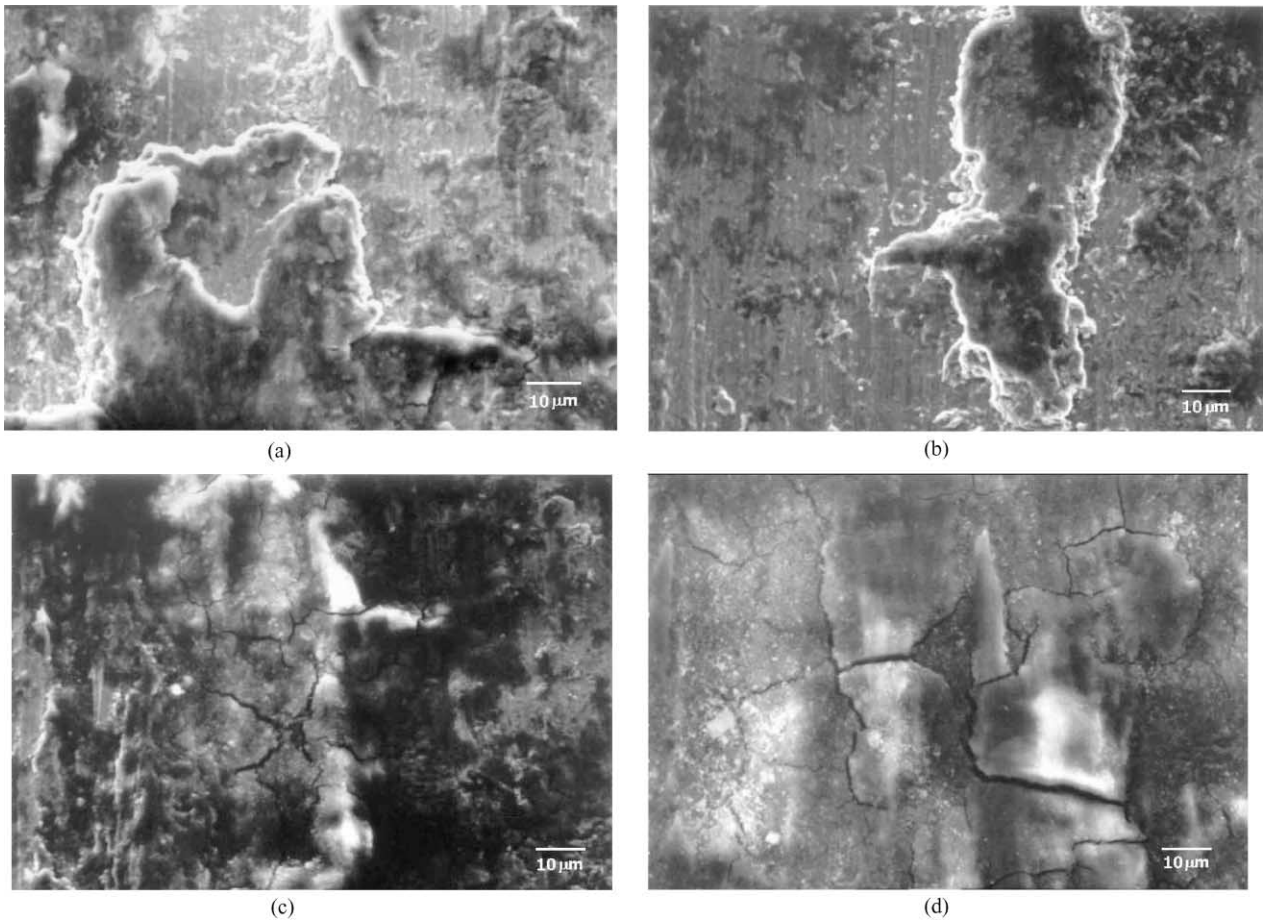

Fig. 5. Results of SEM examination after reciprocating sliding wear tests: (a) Inconel 600MA against 405 ferritic stainless steel; (b) Inconel 600MA against 409 ferritic stainless steel; (c) Inconel 690TT against 405 ferritic stainless steel; (d) Inconel 690TT against 409 ferritic stainless steel.

analysis results showed that they contained a large amount of oxide such as NiO and Cr_2O_3. In the case of the same support materials, the kinds of oxide on the wear particles layer are dependent on the compositions of tube materials. Gawne and Ma [9] showed that Cr_2O_3 is expected to have a much higher interfacial free energy with nickel, producing a low adhesive tendency and wear coefficient. Therefore, it is reasonable to suggest that the high chromium content nickel-base alloy such as 690TT have a low wear rate. To obtain more accurate results, it is necessary to study adhesion behavior between the oxide and the tube materials in details.

3.3. Subsurface deformation behaviors and wear particles

From the above results, it is apparent that wear particle layers play an important role in the reciprocating sliding wear. If these layers are formed at the early stage of sliding, wear rate rapidly decreased. In that, the wear rate difference of tube materials is dependent on the formation of wear particle layers. Consequently, subsurface deformation behaviors are more important because wear particles are generated after severe plastic deformation at contact surface.

Wear particles are generated in initial sliding process. After initial contact between asperities, the contact interface becomes smooth and forms a relatively flat plane. With increasing sliding amplitude and cycles, the degree of surface hardening due to the severe deformation becomes large on the each tube surface. The chemical compositions of 600MA and 690TT are much the same with exception of the chromium contents. Generally, with increasing chromium contents in nickel, stacking fault energy (SFE) of nickel decreases [10]. In the case of low SFE materials, dislocation densities under worn surface during plastic deformation may rapidly increase and work hardening occurs in a short period. Therefore, wear protective layers are rapidly generated on the surface of 690TT that have more chromium contents compared to 600MA.

To verify the subsurface hardening difference with the chromium contents, nano-indentation test were performed at each tube specimens and results show in Fig. 7. From the microhardness (HV) test results, the two tube materials have similar hardness values. But nano-indentation results show that the hardness values in subsurface are much difference and two peak values appeared at each tube materials. Hardness values increased as close with the worn surface and

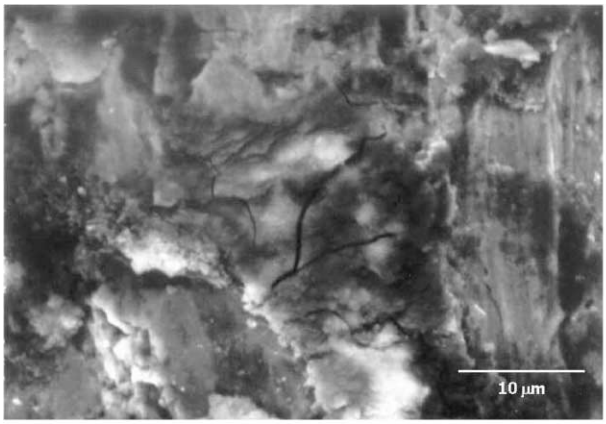

(a)

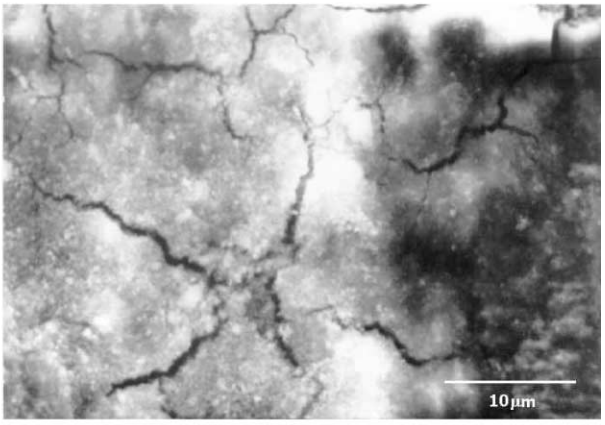

(b)

Fig. 6. Wear particle layers formed during wear testing. In Inconel 690TT, wear particle layers adhere to worn surface even after acoustically cleaning: (a) Inconel 600MA against 405 ferritic stainless steel; (b) Inconel 690TT against 405 ferritic stainless steel.

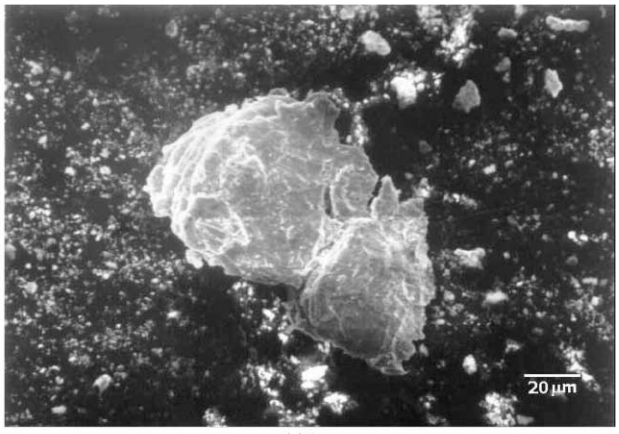

(a)

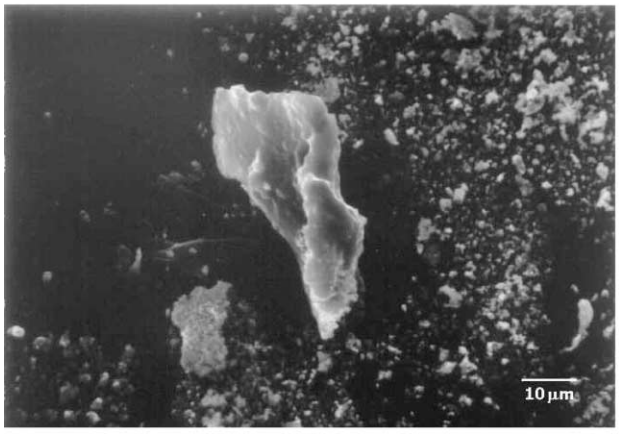

(b)

Fig. 8. Observation results of wear particles using SEM: (a) Inconel 600MA; (b) Inconel 690TT.

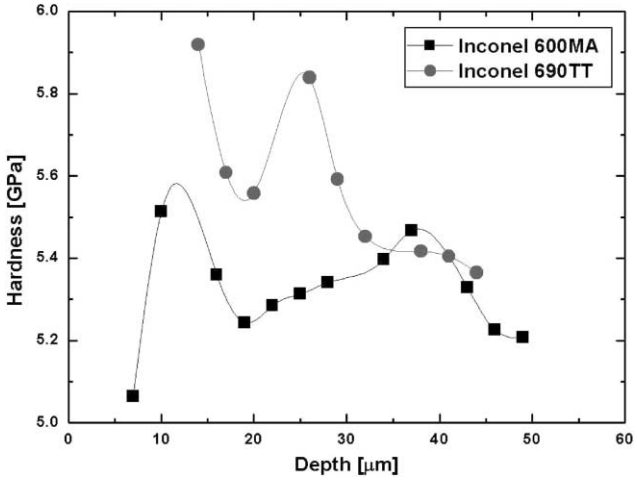

Fig. 7. The results of nano-indentation test. The hardness values in subsurface are much different and two peak values appear for each tube material.

depth appeared first peak are similar at each tube materials. But hardness value near surface in 690TT is high compared with 600MA and second peak depth is more close to the surface in 690TT. Therefore, wear hardening layers that are generated during severe plastic deformation are more wear-protective in 690TT and have influence on the wear particle generation.

The result of wear particle observations in Fig. 8 shows that there is much variation in shape of wear particles. In the case of 600MA, wear particles seem to be generated from the wedges that are formed when surface deformation layers are continuously piled up one on another during repeated shear deformation. On the other hand, ejections of wear particles that are severely deformed on the surface are dominant in 690TT. With increasing sliding cycles, this hardened layer may fracture due to the difference of plastic deformation between surface and subsurface. If shear stress at the contact asperities is high enough to fracture into fragments, deformed layers fracture into several parts on the worn surface and ductile fracture or shear dimple at the eliminated surface is dominant. Besides, these fractured particles further deform with the unfractured layers and are broken into fine particles.

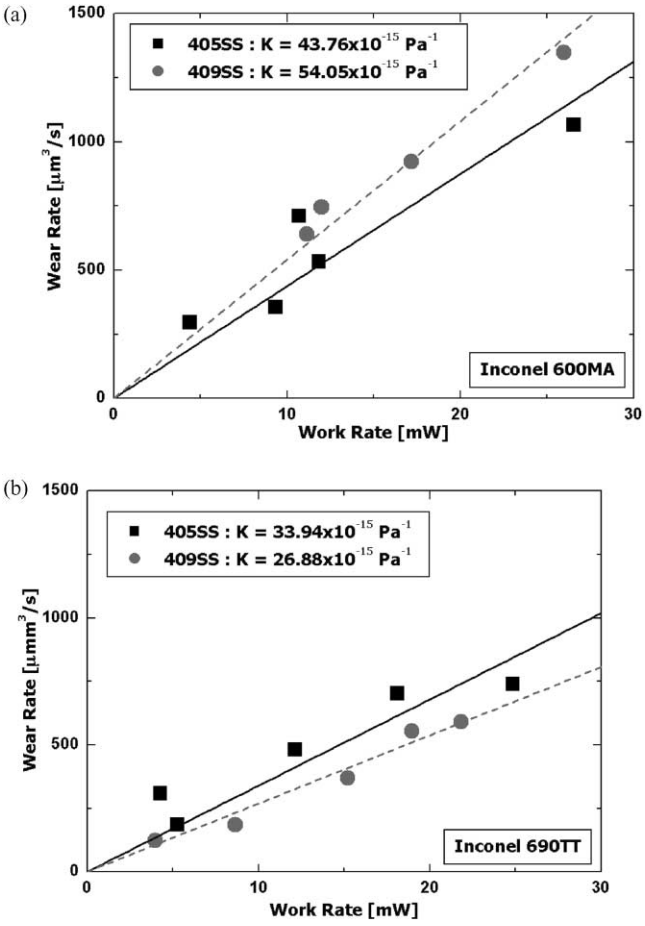

Fig. 9. Calculated wear coefficients from test results. Wear coefficients of Inconel 690TT are low compared with Inconel 600MA: (a) Inconel 600MA; (b) Inconel 690TT.

3.4. Application of the work-rate model

Recently, work-rate model have generally been used as wear model of SG tube materials [11]. This model is based on the Archard wear equation and shows that wear rate increase with increasing sliding amplitude and applied normal load. Wear coefficients of 600MA and 690TT against ferritic stainless steels were estimated by using work-rate model and results are compared in Fig. 9 for work-rate varying from 4 to 30 mW. In 600MA, average wear coefficients are 43.76×10^{-15} Pa for 405SS and 54.05×10^{-15} Pa for 409SS. In 690TT, average wear coefficients are 33.94×10^{-15} Pa for 405SS and 43.76×10^{-15} Pa for 409SS. The results indicate that wear coefficients of 690TT are low compared with 600MA. But the wear rate of two different tube and support combinations could differ by a factor 10, even though their vibration levels are the same. Therefore, for predominantly reciprocating sliding motion, the wear rates of SG tube materials are almost similar regardless of ferritic stainless steels as support materials.

Because of the modification of Archard wear equation, wear coefficient of work-rate model includes material properties such as hardness, deformation characteristics, etc. Especially, it is not always true that relations between hardness and wear volume have an inverse proportion only. Generally, wear volume increases with increasing normal force and sliding distance. These relations could be inferred from the two wear models. Yet, from the experimental results, wear rate transition occurred in 690TT and wear coefficient K is not constant. Attia and Magel indicated that the specific wear coefficient of a full scale multi-span wear test is not constant, but depends on the magnitude of the work rate [12]. Therefore, these calculated values of K have possibilities of underestimating residual life of SG tube. Accordingly, to obtain more accurate wear coefficient, SG wear model must be preponderantly correlated with the mechanism of wear particles generation from hardening layers, the formation of wear particle layers and the ejection mechanism of wear particles from the wear particle layers at each test condition.

4. Conclusions

Reciprocating sliding wear tests were performed using SG tube materials against ferritic stainless steels. From those experimental results following conclusions were obtained.

1. With increasing applied normal load and sliding amplitude, the wear rate rapidly increased in 600MA. But in 690TT, wear transition occurred above the normal load of 15 N and the sliding amplitude of 30 μm.
2. From the worn surface examination, there appeared different wear mechanisms of wear particles between tube materials. The removal of hardened layers generated by ploughing was more dominant in 690TT while wedge formation was dominant in 600MA. It is related to the degrees of deformation strengthening due to the different chromium contents.
3. The load-bearing layers are found in 690TT tube specimen even after specimens were cleaned to remove wear particles in ultrasonic bath for 10 min. But in 600MA, these compacted layers were not found. Therefore, wear particle layers that are generated in 690TT decrease frictions between tube and support materials.
4. Wear transition occurred in Inconel 690TT, but it did not occurs in Inconel 600MA. To obtain more accurate wear coefficient, SG wear model must be preponderantly correlated with the mechanisms of particle generation, particle layer formation and particle ejection at each wear test conditions.

Acknowledgements

This work was partially supported by the Brain Korea 21 project.

References

[1] D.R. Dierchs, et al., Overview of steam generator tube degradation and integrity issues, Nuclear Eng. Design 194 (1999) 19–30.
[2] P.L. Ko, Experimental studies of tube frettings in steam generators and heat exchangers, J. Pressure Vessel Technol. 101 (1979) 125–133.
[3] T.M. Frick, T.E. Sobek, J.R. Reavis, Overview on the development and implementation of methodologies to compute vibration and wear of steam generator tubes, in: Proceedings of the Symposium on Flow-Induced Vibrations: Vibration in Heat Exchanger, Vol. 3, 1984, pp. 149–161.
[4] N.J. Fisher, Experimental fretting-wear studies of steam generator materials, J. Pressure Vessel Technol. 117 (1995) 312–320.
[5] P.L. Ko, M.-C. Toporiat, M. Zbinden, Wear studies of materials for tubes and antivibration bars in nuclear steam generators, J. Pressure Vessel Technol. 118 (1996) 287–300.
[6] F.M. Guerout, Steam generator fretting-wear damage: a summary of recent findings, J. Pressure Vessel Technol. 121 (1999) 304–310.
[7] J. Jiang, F.H. Stott, M.M. Stack, The role of triboparticulates in dry sliding wear, Tribol. Int. 31 (1998) 245–256.
[8] A. Iwabuchi, Role of oxide particles in the fretting wear of mild steel, Wear 151 (1991) 301–311.
[9] D.T. Gawne, U. Ma, Wear mechanisms in electroless nickel coatings, Wear 120 (1987) 125–149.
[10] R.E. Schramm, et al., Stacking fault energies of seven commercial austenitic stainless steels, Metall. Trans. A 6A (1975) 1345–1351.
[11] M.K. Au-Yang, Flow-induced wear in steam generator tubes-prediction versus operational experience, J. Pressure Vessel Technol. 120 (1998) 138–143.
[12] M.H. Attia, E. Magel, Experimental investigation of long-term fretting wear of multi-span steam generator tubes with U-bend sections, Wear 225–229 (1999) 563–574.